Two-Tier Cellular Networks: Secondary Node MIMO Configuration, Applied to LTE-A

Diogo Martins
Instituto Superior Técnico / INOV-INESC
University of Lisbon
Lisbon, Portugal
diogo.s.martins@tecnico.ulisboa.pt

Luis M. Correia
Instituto Superior Técnico / INOV-INESC
University of Lisbon
Lisbon, Portugal
luis.m.correia@tecnico.ulisboa.pt

Elvino S. Sousa
Department of Electrical and Computer Engineering
University of Toronto
Toronto, Canada
es.sousa@utoronto.ca

***Abstract* – The objective of this thesis was to optimize the link between the primary and secondary nodes in a Two-Tier Cellular Network. The optimization was performed as a LTE-Advanced application, by developing a proposed scheme using multiple Modulation Coding Schemes per Resource Block for Link Adaptation. The proposed scheme was obtained from the calculation of the SINR for each Resource Block, differing from the wideband average value in the expected scheme. The throughput gain is evaluated in percentage comparing the proposed and expected schemes. Three frequency selective scheduling algorithms are also evaluated, taking as performance metrics, the fairness improvement, and overall cell throughput gain in percentage. The model is implemented in hardware for data acquisition in the secondary node, and software for channel characterization, link adaptation and scheduler for both nodes. Two scenarios were considered in terms of cell density referring to sparse and dense deployments. An average throughput gain of 10.23 % was obtained for the sparse deployment scenario considering individual reference signals, and 49.35 % for 2x2 MIMO with two arrays of 8 antennas. A fairness improvement of 28.91 %, 80.19 % and 24.13 % and overall cell throughput gain of 63.96 %, 41.15 % and 128.52 % were obtained for the Round Robin, Best CQI and Proportional Fair algorithms. For the dense deployment scenario, one achieved an average of 64.98 % throughput gain, although most of the capture files did not fit the requirements for the correct performance of the proposed scheme, contrary to the sparse deployment scenario.**

Keywords – LTE-Advanced, Two-Tier Cellular Networks, Software Defined Radio, MIMO, RB-dependent AMC, Scheduling.

I. INTRODUCTION

As of 3GPP's Release 10, LTE became known as LTE-Advanced (LTE-A), although they are the same technology. 3GPP determined that the ITU Requirements for 4G would be met with the introduction of LTE-A's new features [1]. LTE-A shares the same network architecture of LTE, however the support of relay nodes (RNs) and heterogeneous networks, such as Two-Tier Cellular Networks, became one of the main technologies under consideration for further 3GPP Releases.

The link between the tiers in a Two-Tier Cellular Network is critical in terms of system optimization because it allows for the use of multiple antennas between the two nodes. To ensure the connectivity for devices, smart access points and user equipment within both cellular network can be simplified by using such wireless backhaul. Additionally, the potential costs for the operators can be minimized, as it is no longer needed a wired backhaul between the multiple terminals, which requires a great investment by the operators [2].

By considering that peaks of traffic form in clusters of users, one can benefit from the hierarchization of a cellular network. By having dedicated nodes serving clusters of users, for example in public transportation and shopping centres, one can guarantee the Quality of Service required in such conditions.

LTE-A's support for Two-Tier Cellular Networks and higher order MIMO systems can be explored to overcome the traffic growth, although they still present some drawbacks in terms of complexity, interference and mobility issues. In a Two-Tier Cellular Network, the communication from a base station, also called a primary node, to end-user equipment occurs through an intermediary station that we refer to as a secondary node.

The scope of this thesis will focus on techniques to optimize this link in terms of secondary node multiple antenna configuration optimizing the link by adopting multiple Modulation Coding Schemes (MCS) per resource block for Adaptive Modulation and Coding (AMC). The secondary node is implemented in hardware for data acquisition using the prototyping platform MegaBEE [3] and its main functionalities in terms of channel characterization in software using MATLAB. The main output of this work is that the optimization undertaken presents a great throughput improvement, however it is too dependent on the radio channel steady conditions.

This report is composed of 6 Sections including the present one. Section II presents the fundamental concepts regarding LTE-A networks, and Two-Tier Cellular Networks, finalizing with a review of state of the art related works. The model to be developed to optimize the link of the primary and secondary nodes of a Two-Tier Cellular Network is presented in Section III, including its description, the theoretical aspects related to the model and the performance parameters to analyze. Section IV pertains to the model implementation both in Software and Hardware and its preceding assessment to evaluate the correct functionality. The results analysis is demonstrated in Section V for the introduced scenarios in this section. To conclude, in Section VI, the main conclusions of this paper are evaluated, with the addition of further improvements for future work.

II. Fundamental Concepts and State of the Art

A. LTE-Advanced

The addressed topics in this subsection are the result of an adaptation of the works of [4].

There are 4 main components in LTE's system architecture namely the Services, the EPS composed of the Evolved Universal Terrestrial Radio Access Network (E-UTRAN) and the Evolved Packet Core (EPC), and finally the User Equipment (UE). In terms of functionality, the 4 main components have distinct roles in the system architecture.

In DL, the technique used to handle multiple access is Orthogonal Frequency Division Multiple Access (OFDMA), which is a suitable solution to handle high data rates, possessing low sensitivity to interference and fast fading, and a reduced control information overhead. In LTE, the physical resource that is allocated to a user is known as a Resource Block (RB). A RB is composed in frequency by 12 sub-carriers, spaced by 15 kHz, and in time by 1 slot with the duration of 0.5 ms.

In UL, contrary to OFDMA which works with separated transmitted subcarriers, Single Carrier Frequency Division Multiple Access (SC-FDMA) works with jointly transmitted subcarriers. This means that each symbol in SC-FDMA is not assigned to a subcarrier like OFDMA.

Other than the network architecture support for RNs and heterogeneous networks, LTE-A introduced new improvements in the radio interface. The major improvements were the increase of bandwidth (which leads to a higher capacity), coverage, quality of service, network utilization and interference management using Carrier Aggregation (CA), Coordinated Multipoint (CoMP) and multiple antennas enhancement techniques.

B. Two-Tier Cellular Networks

The concept of a Two-Tier Cellular Network refers to a hierarchy-based cellular network where low power nodes, such as small cells and relay nodes, are distributed throughout the conventional macro cellular network. The first tier of this hierarchy-based architecture is referred as primary node for a macro-cell where, the secondary node tier comprises both small cells and relay nodes.

Two-Tier Cellular Networks provide a higher coverage and capacity to the surrounding users at the cost of an increased interference. In this type of networks, interference emerges not only from neighbouring cells (co-tier interference) in the primary node tier but also from the secondary node tier (cross-tier interference).

Techniques ranging from power control to resource allocation [5] can be considered to mitigate the added effects of interference in this type of networks. The deployment growth of Two-Tier Cellular Networks, not only leads to interference issues but also to mobility ones.

Mobility management emerges to solve the typical events that cause this break in Quality of Service (QoS), such as handover failures, radio link failures and unnecessary handovers, also referred as ping-pong events [6]. On the other hand, even if the mobility is handled properly, by successfully completing a handover, there is an increasing load in the network due to how frequent handovers occur.

The densification of small cell areas introduces the need of a more efficient backhaul such that the network traffic can be dealt with in an appropriate way. The deployment of a backhaul network for Two-Tier Cellular Networks, must overcome a set of challenges to provide a cost-effective solution while guaranteeing the QoS needed. The challenges reside mostly on the overall quality of the link [7], regarding coverage, capacity and synchronization, but also with the physical design and hardware architecture and at last the costs to assess the backhaul solution.

C. State of the Art

In this section, the state of the art regarding Massive MIMO deployments considering multiple antennas at both transmitter and receiver is evaluated. These types of links can be applied in a Two-Tier Cellular Network for backhaul and antenna offloading, to achieve a more balanced network.

The works of [8], proposes a TDD based network architecture where a Massive MIMO base station BS is overlaid with a dense tier of small cells. The authors compare two duplexing schemes, TDD and Reverse-TDD, being that the former reverses the order of downlink and uplink periods in one of the tiers. The simulation results indicate that the proposed scheme can significantly minimize the aggregate cross-tier interference experienced by small cells at the price of a negligible macro performance loss.

In [9] it is proposed a novel moving cell to provide an adequate resource management and overcome the challenges emerged from group mobility, namely, where many UEs share the same moving platform such as public transportation. The proposed solution is thus an evolution of a mobile relay node deployed on the moving platform.

Applying Massive MIMO, with 256 antenna elements in the transmitter and 64 in the receiver, for backhaul connection and LTE-A Rel.10 relay architecture for the baseline of the moving cell it was studied the performance of the backhaul capacity in terms of horizontal and vertical distance from the base station. It was shown that the system's capacity was significantly increased when compared to the conventional macro cell approach, even though it varies periodically. The total number of control signal overheads are also reduced in the moving cell, when compared to the macro cell, thus improving the user Quality of Experience (QoE).

III. Model Development and Performance Parameters

A. Model Description

The proposed scheme aims to take advantage of the overall properties of a secondary node when compared to a regular UE. The secondary node model employed in this analysis is static thus the channel impulse response is expected to be steady without drastic changes along time. By employing multiple antennas at the secondary node, one can achieve higher modulation coding schemes improving the capacity of the system. With these conditions, the procedure of AMC using

independent MCS in assigned RBs can be considered as a valid option to improve the link between the primary and secondary node

To reduce the signalling overhead created by adopting multiple modulation coding schemes per resource block, the proposed scheme determines a SINR threshold according to the measured CQIs of the first demodulated slot of a LTE frame, applying the same MCSs for the following slots. Sudden changes in the channel behaviour will result in the update of the MCS to be adapted for the following slots proceeding the fluctuation.

The model for the proposed scheme is presented in Fig. 1. The model can be defined in two layers, the secondary node layer and the primary node layer. In the first mentioned layer, the secondary node has captured related parameters in what concerns the number of antennas and diversity type, its surrounding environment for its deployment site and its behavior according to mobility.

From these input parameters, the secondary node will collect LTE signals data from several base stations, performing its demodulation and determining the CQI index to report to the primary node based on the measured SINR. The reported CQI indices are from both the proposed scheme and expected one, considering respectively an independent and common RB Modulation Coding Scheme. From the several captures, the primary node layer will perform the action of link adaptation and scheduling which in turn will provide the performance parameters taken for analysis.

B. Secondary Node Receiver Development

The first module to be implemented in the secondary node is its data acquisition system. The equipment used to collect data is the FPGA-based Software Defined Radio platform MegaBEE [10]. MegaBEE comprises two subsystem units for the left and right side of this platform being that each subsystem unit is composed by one baseboard and two RF frontend boards. The baseboard has as its main component an all programmable System on Chip Zynq device (Z7100) from Xilinx containing a dual ARM Cortex-A9 processor as its processing system (PS) and as programmable logic (PL) a fabric which is equivalent to a Kintex-7 FPGA. To program the FPGA a bit-stream file is created in Simulink using BEECube Platform Studio (BPS) [11].

Three methods are used to transfer received data from the MegaBEE to a host computer. The methods are from now referred as Block RAM (BRAM) Method, Direct Memory Access (DMA) Method and 10 GbE (XGE) Method with each method name referring to a main BPS block.

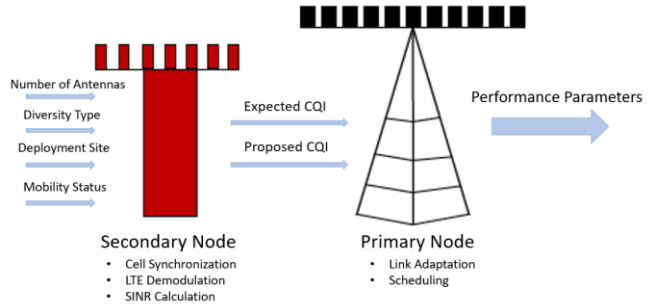

Figure 1 – Model Structure.

The BRAM method consists of storing the RF signals from each port to a set of Shared Block RAMs. Each BPS BRAM block can store a maximum of 2^{15} samples, being an implementation of 32 Xilinx Shared BRAMs. Due to the hardware constraints, there is a limited number of BRAM blocks from BPS that can be used, decreasing the total number of samples that can be obtained using this method.

The DMA method, makes use of a Direct Memory Access to transfer data from the programmable logic to the processing system of the chipset.A DMA transfer is based on two asynchronous First-In First-Out (FIFO) buffers, one for the PS and the other for the PL. The data is then stored in the DDR3 DRAM, which can be accessed by software in the PS and hardware in PL.

Following the AXI-4Stream protocol [12], a DMA transfer occurs when the transferred data and the FIFO is ready to be written, by asserting two hardware flags, TREADY and TVALID, at the same time, given that the boundary of the transferred data needs to be known in order to indicate the last beat of the transfer to the PS, by asserting an additional hardware flag, TLAST.

The last used method to acquire data in a continuous way consists of transmitting a stream of RF data from all the ports over a 10 GbE (XGE) connection between a host processor and the SFP+ outputs in the MegaBEE [13]. From the MegaBEE side, the stream of data consists of a UDP packetization of two RF ports from the FMC-112 board with a variable payload length.

For a sampling frequency of 30.72 Msamples/s, a comparison of the three data acquisition methods can be found in Table I.

TABLE I. DATA ACQUISITION METHODS COMPARISON.

Method	BRAM	DMA	XGE
Number of Antennas	4	4	4
Captured Samples	~100 000	~500 000	Unlimited
Delay between captures	Order of seconds	Order of milliseconds	Continuous
Gaps within capture	Non-existent/Not identified	Non-existent/Not identified	Dependent on host performance

With the acquired data, the secondary node proceeds to perform the channel characterization. The procedure prior to the demodulation of a LTE signal aims to the estimation of the carrier frequency offset value and also to obtain synchronization by acquiring the information on the connected cell regarding its cell identifier, cyclic prefix length and duplexing mode in order to determine the offset between the beginning of the captured data and the start of a LTE frame. After this procedure is finished the full demodulation can be performed by retrieving the number of cell-specific reference signal ports and bandwidth in terms of number of resource blocks.

Following the cell synchronization and LTE demodulation is the procedure of AMC. AMC works by measuring and feeding back the channel SINR to the transmitter, which then chooses a suitable MCS from a "code set" to maximize throughput at that SINR. The CQI parameter is determined by the secondary node and can be directly mapped according to certain ranges of experienced Signal-to-Noise-plus-Interference Ratio for a Block Error Rate (BLER) of 10%.

The mapping of the CQI indices in terms of MCS, coding rate and spectral efficiency can be observed in Table 7.2.3-2 from [14]. The mapping in terms of SINR value is given according to the tabulated spectral efficiency values in [14], for a modulation coding scheme up to 256-QAM as LTE-A already has support for this modulation order, being based on a truncated Shannon limit formula found in [15] given by:

$$C_{c[\text{bit/s/Hz}]} = \begin{cases} 0 & , \text{ for } \rho_{IN[\text{dB}]} < \rho_{IN,\min[\text{dB}]} \\ \alpha S(\rho_{IN[\text{dB}]}), & \text{for } \rho_{IN,\min[\text{dB}]} \le \rho_{IN[\text{dB}]} \le \rho_{IN,\max[\text{dB}]} \\ C_{c,\max[\text{bit/s/Hz}]} & , \text{ for } \rho_{IN[\text{dB}]} > \rho_{IN,\max[\text{dB}]} \end{cases} \quad (1)$$

Where:

- ρ_{IN} : Signal-to-Noise-plus-Interference Ratio;
- $S(\rho_{IN}) = \log_2(1+\rho_{IN})$;
- $\alpha = 0.75$.

The minimum and maximum values of SINR can be calculated by knowing the respective spectral efficiency for the highest and lowest CQI index. By replacing the tabulated spectral efficiency values from [14] in (1), a range of SINR is obtained for each CQI index, allowing the mapping of each index in terms of the SINR value measured at the UE. This mapping can be used to shows which modulation coding scheme and coding rate is employed by CQI index according to the calculated SINR range.

C. Performance Parameters

The measured SINR at the receiver is calculated based on Cell-Specific Reference signals transmitted power in DL from the connected cell and surrounding interfering cells. Cell-Specific Reference Signals position depends on the number of antennas used at the transmitter and the cell-ID determined during the synchronization procedure.

To apply different modulation coding schemes, the SINR value must be calculated for each resource block within a given period of time. After LTE demodulation, one has already obtained a resource grid in terms of OFDM symbols and sub-carriers for all received resource elements.

The mapping of cell-specific reference signals in this grid can be used to determine the received power per resource block according to the number of antennas used on the transmitter. Although it does not transmit any specific information, it can deliver a reference point to the DL power transmitted by the eNB. The sequence format is defined in clause 6.10.1.1 in [16].

The received power per resource block for a given cell-ID can be calculated as the average squared magnitude of cell-specific reference signals contained in the resource block:

$$P^{ID}_{r,RB_{[\text{W}]}} = \left| \overline{r^{(p)}_{k,l} a^{*(p)}_{k,l}} \right|^2 \quad (2)$$

Where:

- $r^{(p)}_{k-CRS,l-CRS}$: Received demodulated value of cell-specific reference signal mapped on resource element $(k-CRS, l-CRS)$ for antenna port p;
- $a^{(p)}_{k-CRS,l-CRS}$ Value of cell-specific reference signal mapped on resource element $(k-CRS, l-CRS)$ for antenna port p.

When performing the average for all the demodulated reference signals, fluctuations can occur within the individual RBs along a slot. To reduce the fluctuations that can be experienced along the different RBs along the slot, an alternative method is proposed where a single reference signal is considered to measure the received power. The reference signal numbering for different number of transmitting antennas can be found in Fig. 2.

To calculate the SINR one must first determine the received power from each interfering cell is obtained in a similar manner as the connected cell. The noise power level is assumed to be generated from thermal noise as the system can be considered interference-limited.

By determining the received power per resource block from the connected cell and interfering cells, and calculating the noise power level considering MegaBEE receiving front-end noise factor N_f, the SINR value, $\rho_{IN,RB}$, is given by:

$$\rho_{IN,RB_{[\text{dB}]}} = 10\log_{10}\left(\frac{P^{ID_c}_{r,RB_{[\text{W}]}}}{\sum_{i \neq c} P^{ID_i}_{r,RB_{[\text{W}]}} + N_{RF,RB_{[\text{W}]}}} \right) \quad (3)$$

Where:

- $P^{ID_c}_{r,RB_{[\text{W}]}}$: Received power per resource block of connected cell;
- $P^{IDi}_{r,RB_{[\text{W}]}}$: Received power per resource block of interfering cell;
- $N_{RF,RB_{[\text{W}]}} = k_{B_{[\text{J/°K}]}} T_{[\text{°K}]} \Delta f_{RB_{[\text{Hz}]}} N_f$, for $T_{[\text{°K}]} = 290\,\text{°K}$ $k_{B_{[\text{J/°K}]}} = 1.38 \times 10^{-23}\,\text{J/°K}$, and $\Delta f_{RB_{[\text{Hz}]}} = 18\,\text{MHz}$.

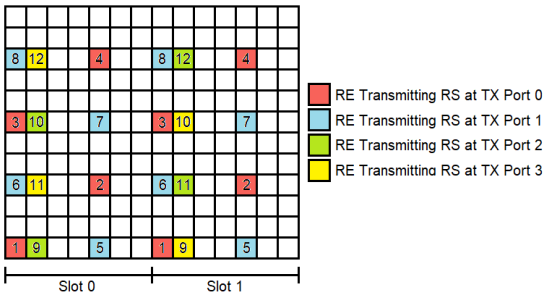

Figure 2 – Reference Signal Numbering.

From the measured SINR value, the spectral efficiency can be directly determined by mapping the obtained value to the calculated SINR range, thus selecting which CQI index the UE/secondary node sends to the eNB and which modulation coding scheme is used. the throughput per resource block is simply given by the product of this value with the bandwidth a resource block occupies which is 12 sub-carriers spaced 15 kHz apart totalling a 180 kHz bandwidth.

The total throughput for a given slot can then be calculated as the sum of the individual throughputs of the total resource blocks for the whole bandwidth. This throughput can be considered optimal as all the resource blocks have an associated modulation coding scheme, being given by:

$$R_{b,s[\text{bit/s}]}^{opt} = \sum_{i=1}^{N_{RB}^{DL}} R_{b,RB_i[\text{bit/s}]} = \sum_{i=1}^{N_{RB}^{DL}} C_{c,RB_i[\text{bit/s/Hz}]} \Delta_{f,RB[\text{Hz}]} \quad (4)$$

Where:

- R_{b,RB_i} : Individual throughput per resource block;
- C_{c,RB_i} : Individual spectral efficiency per resource block after MCS selection.

To reduce the signaling overhead created by adopting multiple modulation coding schemes per resource block, the proposed scheme determines a SINR threshold according to the measured CQIs of the first demodulated slot of a LTE frame, applying the same MCs for the following slots. Sudden changes in the channel behavior will result in the update of the MCS to be adapted for the following slots proceeding the fluctuation. The actual optimal individual throughputs as follows:

$$R_{b,RB_i[\text{bit/s}]}^{act-opt} = \begin{cases} R_{b,RB_i[\text{bit/s}]}, \text{ for } \rho_{IN,RB_i[\text{dB}]} \geq \rho_{IN[\text{dB}]}^{s_1} \\ 0 \quad , \text{ for } \rho_{IN,RBi[\text{dB}]} < \rho_{IN[\text{dB}]}^{s_1} \end{cases} \quad (5)$$

The actual optimal throughput per slot would then be given by:

$$R_{b,s[\text{bit/s}]}^{act-opt} = \sum_{i=1}^{N_{RB}^{DL}} R_{b,RB_i[\text{bit/s}]}^{act-opt} \quad (6)$$

In the expected scheme, the MCS is based on the wideband SINR resulting from the average or sub-band average measured received power, thus a single throughput or sub-band throughput is achieved for the assigned resource blocks. The average SINR can be formulated as:

$$\overline{\rho_{IN_{[\text{dB}]}}} = 10\log_{10}\left(\frac{\overline{P_{r,RB_{[\text{W}]}}^{ID_c}}}{\sum_{i \neq c} \overline{P_{r,RB_{[\text{W}]}}^{ID_i}} + N_{RF,WB_{[\text{W}]}}} \right) \quad (7)$$

The difference between (7) and (3) is not only in terms of the average received power per resource block being used as inputs, but also how the noise power level is determined for the whole bandwidth. The expected throughput per slot is given by:

$$R_{b,s[\text{bit/s}]}^{\exp} = \overline{C_{c,s}}_{[\text{bit/s/Hz}]} \Delta_{f,s[\text{Hz}]} \quad (8)$$

Where:

- $\overline{C_{c,s}}$: Average spectral efficiency measured in a slot;
- $\Delta_{f,s}$: Transmitted DL signal bandwidth.

For the average throughput, a single Modulation Coding Scheme is selected based on the average SINR (7), creating a threshold for the actual throughput. Considering the threshold effect on the calculated individual throughputs, the actual individual throughput is determined as follows:

$$R_{b,RB_i[\text{bit/s}]}^{act} = \begin{cases} R_{b,RB[\text{bit/s}]}^{avg}, \text{ for } \rho_{IN,RB_i[\text{dB}]} \geq \overline{\rho_{IN}}_{[\text{dB}]} \\ 0 \quad , \text{ for } \rho_{IN,RBi[\text{dB}]} < \overline{\rho_{IN}}_{[\text{dB}]} \end{cases} \quad (9)$$

Where $R_{b,RB}^{avg}$ is calculated for the average spectral efficiency $\overline{C_{c,s}}$ measured in a slot for a resource block bandwidth $\Delta_{f,RB}$.

The same procedure in (6) is applied to determine the actual throughput per slot as:

$$R_{b,s[\text{bit/s}]}^{act} = \sum_{i=1}^{N_{RB}^{DL}} R_{b,RB_i[\text{bit/s}]}^{act} \quad (10)$$

To observe the performance improvement of the proposed scheme in regard to the expected scheme, the throughput gain is calculated from the difference between the actual optimal throughput from (6) and actual throughput from (9) as:

$$G_{b,s[\%]} = \frac{(R_{b,s[\text{bit/s}]}^{act-opt} - R_{b,s[\text{bit/s}]}^{act})}{R_{b,s[\text{bit/s}]}^{act}} \times 100 \quad (11)$$

Each measured throughput can be enhanced by applying multiple antennas techniques. The MegaBEE equipment to be used in this thesis supports 8 antennas, being that there is two MegaBEEs available to perform the measurements. The total number of 16 antennas are considered for two multiple antenna techniques, combining diversity and MIMO.

For the experiments, two arrays of 8 antennas with each element spaced half of a wavelength apart in the configuration presented in Fig. 3.

The combining diversity algorithm considered can be implemented, as the combined signal grid of RBs and slots is formed by choosing the maximum SINR measured at each antenna. The SINR grid in a RB *n* in slot *t* when considering this diversity combining algorithm can thus be defined as:

$$\rho_{IN,n,t\ [\text{dB}]}^{div} = \max \rho_{IN,n,t\ [\text{dB}]}^{(p)} \quad (12)$$

Where:

- $\rho_{IN,n,t}^{(p)}$: Measured SINR in RB *n* in slot *t* for antenna port .

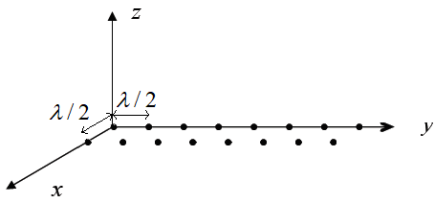

Figure 3 – Antenna array configuration.

The calculation of the expected throughput and optimal throughput and corresponding actual throughputs would then consider the SINR grid created from the combining diversity to determine the CQI index to report to the eNB. Considering combining diversity the throughput is calculated on an analogous manner as:

$$G_{b,s[\%]}^{div} = \frac{(R_{b,s[\text{bit/s}]}^{act-opt_{div}} - R_{b,s[\text{bit/s}]}^{act_{div}})}{R_{b,s[\text{bit/s}]}^{act_{div}}} \times 100 \quad (13)$$

For MIMO the two arrays of eight antennas are used to mimic two receivers to employ 2x2 MIMO. The throughput gain would then change to:

$$G_{b,s[\%]}^{MIMO} = \frac{(R_{b,s[\text{bit/s}]}^{act-opt_{MIMO}} - R_{b,s[\text{bit/s}]}^{act_{MIMO}})}{R_{b,s[\text{bit/s}]}^{act_{MIMO}}} \times 100 \quad (14)$$

To evaluate the performance of the three scheduling algorithms, other than overall cell throughput given by the sum of all the secondary nodes throughput, the fairness along slots is calculated. The fairness is measured according to Jain's fairness index being calculated for each slot as:

$$F_{index} = \frac{\left(\sum_{i=1}^{N_{\text{sec}nodes}} R_{b_i[\text{bit/s}]} \right)^2}{N_{\text{sec}nodes} \sum_{i=1}^{N_{\text{sec}nodes}} R_{b_i[\text{bit/s}]}^{\ 2}} \quad (15)$$

Where:

- R_{b_i} : Throughput of secondary node *i*;
- $N_{\text{sec}nodes}$: Number of secondary nodes to be scheduled.

IV. Model Implementation and Assessment

The four modules for the model implementation and subsequent integration are described in Fig. 4.

The first module of the model is the receiver configuration. The three methods for data acquisition were implemented in Simulink by creating a model with the BPS distribution and Vivado System Generator for DSP libraries, to generate a bit-stream to program the FPGA. In a remotely controlled remote shell one then proceeds to configure the transceiver in the MegaBEE.

The second module refers to signal processing with the acquired data, namely in terms of cell synchronization, carrier frequency offset correction, performing after demodulation this processing phase. This analysis is done in MATLAB using LTE's System Toolbox [17] based on the example for Cell Search, MIB and SIB1 Recovery [18]. This step will provide a synchronized demodulated grid in terms of OFDM symbols and subcarriers and the cell-id from which capture was synchronized to.

The demodulated grid and cell-ids will be used in the third module to perform the calculation of the performance parameters for the proposed and expected scheme. For the synchronized cell and interfering cells, the SINRs are calculated and mapped to CQI index to determine the throughput for both proposed and expected schemes. The throughputs obtained in the third module will be used to apply three scheduling algorithms in the fourth module, finalizing with a comparison between each scheduling algorithm.

The scheduling algorithms used in the analysis were all implemented in MATLAB according to their known definitions, however adapted for a scheduler on a resource block level and subband level. Several tests were performed on the four modules that compose the final model, being done in a sequential way, meaning that only when a module was completely tested and assessed its functionality, that the following module was tested.

For the first module regarding the data acquisition methods in the MegaBEE, simulations are performed to the several subsystems for each method. The chosen method was the DMA based one given that although the simulations in all three methods behave as expected, the BRAM and XGE Methods in practice do not offer the flexibility of the DMA Method, being either from the capture delay and reduced number of captured samples in the former and package loss rate in the latter.

The second module is tested by performing the demodulation and cell synchronization on the generated .txt files with the received data. To assess the functionality of this module, the obtained information from demodulation procedure is compared against the one measure in Iphone's embedded Test Field Mode [19], obtaining matching results thus proving the validity of the second module algorithms.

As the third module refers only to the calculation of the performance parameters for the proposed scheme, its functionality is assured by performing simple tests pertaining to the validity of the employed data structures and validity of the demodulated data in all antennas.

The assessment of the fourth was done with simulated data. Two secondary nodes are scheduled using the full totality of resource blocks to allocate with different channel conditions. In the Best-CQI algorithm an over-allocation was observed for the user with the best channel conditions, and a fairer output for the Round Robin algorithm compared to Proportional Fair one, although the latter had a higher cell throughput.

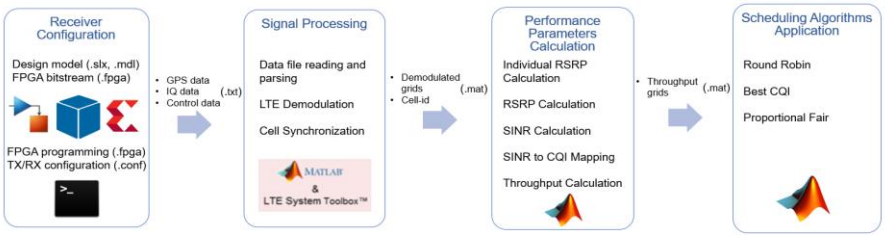

Figure 4 – Model Workflow.

V. Results Analysis

A. Scenarios

The scenario location takes place in the city of Toronto, in particular, the University of Toronto St George Campus and its surroundings. An initial run to gather several captures using DMA Method for data acquisition, was performed for further analysis in terms of cell synchronization, allowing to perform an estimation of the coverage area of the environment cells.

Recordings of the Iphone's Test Field Menu were done in parallel to obtain the Tracking Area Code, Cell Identity and Physical Cell-id of each cell. These parameters were then used to gather an estimation of the location of the base stations using an online application for cell location, LocationAPI [21].

As presented in Fig. 5, a big marker corresponds to a eNB while a small marker refers to a DMA capture. A DMA is synchronized to a given eNB when a small marker shares the same color as a green marker. Also in Fig. 5, one defined the two scenarios under analysis. In green, the sparse deployments scenario A and B have up to 3 cells within a radius of 500 m. In red, the dense deployments C and D have more than 3 cells within the same radius. The center of each circle is located on the same location of a capture used for the analysis.

The measured radio channel belongs to LTE band 7, with a central carrier frequency of 2.630 GHz, a bandwidth of 20 MHz with the transmitter having two antennas in its setup. The receiver configuration is within a plywood case being at the top of a vehicle with a height of 1.44 m as seen in Fig. 6. The receiver consists of two MegaBEEs comprising sixteen antennas for the RF frontend and four antennas to acquire the GPS coordinates. The used equipment comprised 132169 Amphenol RF Division SMA connectors, TG.10.0113 Triton dipole Antennas, and RG316 SMA Cables.

Prior to the measurements, a calibration of the MegaBEE was undertaken in terms of the offset between its receiver local oscillator and measured carrier frequency. Using the signal generator HPE4432B a sinusoidal wave with a carrier frequency of 2.630 GHz was generated and fed to one of the RF ports inputs of the MegaBEE.

By tuning the voltage level fed to auxiliary DAC (AUXDAC2) of the MegaBEE, one could calibrate the receiver local oscillator and thus minimize the frequency offset. The minimum frequency offset value was obtained for an AUXDAC voltage level of approximately 1320 mV.

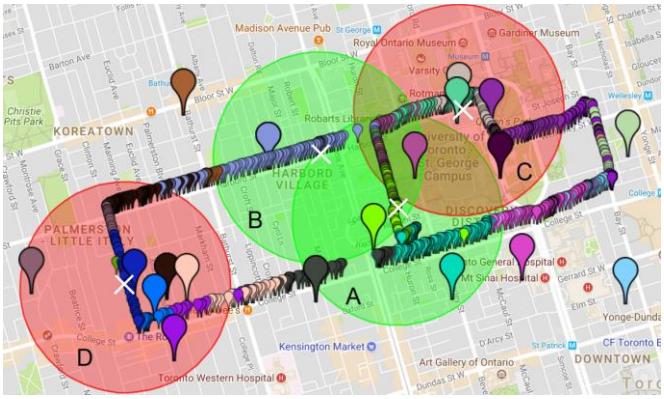

Figure 5 – Sparse and Dense Deployments.

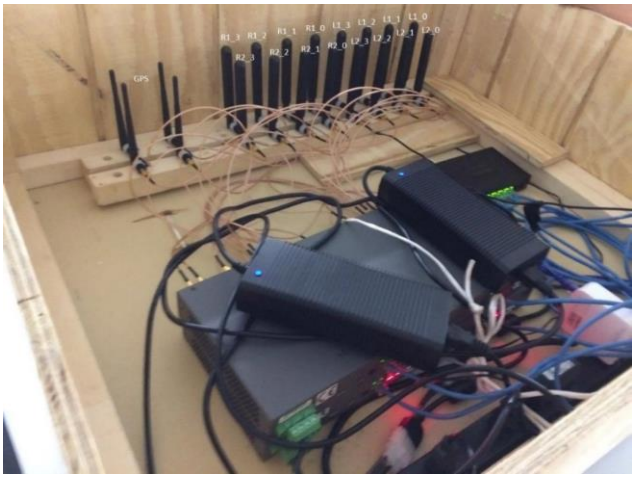

Figure 6 – Equipment setup.

B. Sparse Deployment Scenario Results

The results obtained for the sparse deployment scenario refer to the 30 captures performed at the crossroad of Russel and Huron streets. The capture site can be seen in Fig. 7, along with the closest cells within a radius of 500 m. In terms of synchronization, all the 30 captures are synchronized to the eNB with the physical cell- ID 117 (green).

For the SINR calculation, only two eNBs are considered as interferers for being the closest cells to the capture site, with the cell-IDs, 121 and 276. As the reference scenario defined a radius of 500 m for the sparse deployment scenario, the possible interference created by the cells not contained in this radius is not taken into consideration in this analysis.

Since the analysis deals with real network measurements, possible variations on the expected results can occur with the possibility of being aggravated by the imperfections of the measuring equipment. A filtering of the different files was

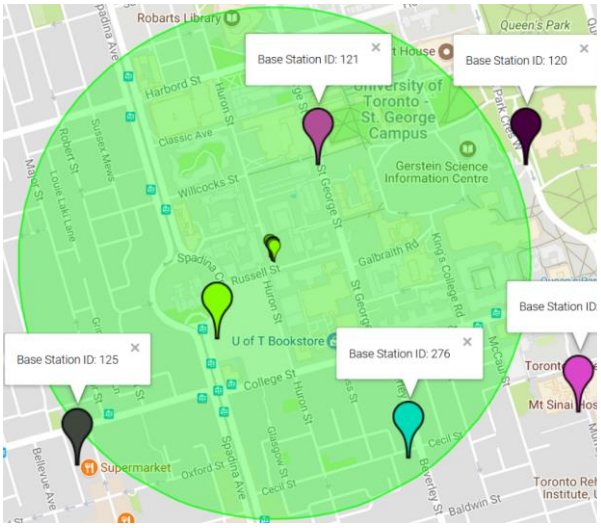

Figure 7 – Sparse Deployment Scenario.

performed aiming to categorize the different behavior obtained when the model is applied to each capture:

- **Category 1:** Constant Expected Throughput;
- **Category 2:** Optimal Throughput is greater than Expected Throughput;
- **Category 3:** Actual Optimal Throughput is greater than Actual Throughput.

The first phase of the analysis went through all the capture files to determine the performance parameters and assess their behavior, focusing on the calculation of the performance parameters with received power being calculated as the average of the reference signals within each resource block. This analysis was undertaken for just the antenna port labelled L1_0.

From the 30 captured files, 26 belong to Category 1 (86.7 %), 1 to Category 2 (3 %), and 9 to Category 3 (30 %). Most of the captured files are within Category 1 and Category 3 which overall indicates a small variation on the radio channel behavior and a potential performance gain for the proposed scheme.

Eight files belong to both Category 1 and Category 3, which indicates that although there is a throughput gain for the proposed scheme over the actual measured throughput, by performing the average to calculate the received power per resource block, the full potential of using individual MCS is not yet achieved. In Fig. 8 one can see the example of the behavior in one of the capture files.

The summary of throughput gain is presented in Table II.

TABLE II. SPARSE DEPLOYMENT THROUGHPUT GAIN RESULTS FOR AVERAGE REFERENCE SIGNALS.

	μ	**σ**	**MAX**	**MIN**
$R^{G}_{b,s[\%]}$	5.24	1.39	8.08	0.34

By performing the average on all the reference signals, possible fluctuations on a single reference signal can originate the fluctuations on the measured optimal throughput causing the additional schemes to be affected as well. The received power per resource block is thus calculated based on the individual reference signals. The alternative method that was undertook to measure the received power per resource block resorted to individual reference signals within the resource block.

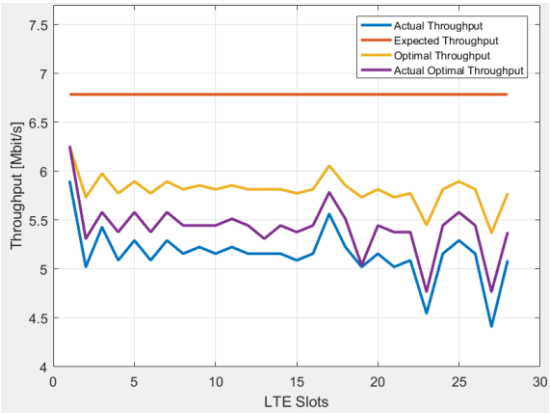

Figure 8 – Sparse Deployment Throughput Curves for Average Reference Signals.

There was a general increase of the percentage of files belonging to the three categories, when considering individual reference for the received power per resource block calculation. From the 30 captured files, 13 (43.3 %) are inserted into the three categories for at least two reference signals. The 7th reference signal within the resource block had the best performance, with its performance being presented in Fig. 9.

The summary of the throughput gain for the individual reference signal RS_7 is presented on Table III.

TABLE III. SPARSE DEPLOYMENT INDIVIDUAL REFERENCE SIGNAL RS_7 PROPOSED SCHEME PERFORMANCE.

	μ	**σ**	**MAX**	**MIN**
$R^{G}_{b,s[\%]}$	10.23	10.02	48.61	-1.05

The maximum gain for each array is obtained for the first slot, when the actual throughput is equal to the optimal throughput. Due to the optimal throughput employing individual MCS for each resource block, it is highly greater than the actual throughput explaining the high percentage gain which is observed.

To improve the performance of the proposed scheme, while still considering the individual reference signals for received power calculation, is the use of antenna diversity. Two antenna arrays are thus considered:

- **Array 1:** Ports L1_0, L1_1, L1_2, L1_3, R1_0, R1_1, R1_2 and R1_3;
- **Array 2:** Ports L2_0, L2_1, L2_2, L2_3, R2_0, R2_1, R2_2 and R2_3.

The overall trend is that the actual throughput tends to be equal to the expected throughput. This will lead that the actual throughput, given that it is calculated by the sum of components which are more likely to be above the threshold imposed by the expected throughput. Considering diversity, the reference RS_3 had the best performance with the summary of the throughput gain being presented in Table IV for the two arrays and MIMO.

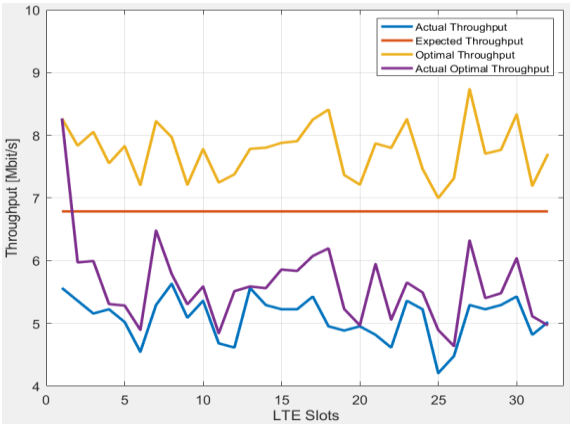

Figure 9 – Sparse Deployment Throughput curves per slot for Individual RS_7.

TABLE IV. DK SPARSE DEPLOYMENT THROUGHPUT GAIN RESULTS FOR DIVERSITY COMBINING IN RS_3.

		Array 1	Array 2	MIMO
$R^{G}_{b,s[\%]}$	**μ**	80.90	16.75	49.35
	σ	18.01	10.52	13.73
	MAX	149.57	60.77	105.85
	MIN	44.56	3.18	24.70

In terms of the MIMO results, one observes that the throughput gain is not as high relative to Array 1. This is explained by the fact that the by the optimal throughput being the result of the sum rate of the two arrays with MIMO, the expected throughput will increase as well as the actual throughput. Nonetheless, the obtained results match the expected in a typical 2x2 MIMO configuration, with an increase of the capacity by the order of the minimum number of antennas employed at the receiver or transmitter.

For the scheduling algorithms, to compare the improvements of the proposed scheme compared with the expected scheme, a subband reporting is considered where the secondary node reports the average CQI for *k*-sized subbands. The subband size *k* in resource blocks, for a bandwidth of 20 MHz, is 8 resource blocks [14] thus comprising 12 subbands within the whole LTE bandwidth.

Five secondary nodes are considered for scheduling. The first secondary node, with the worst channel conditions, performs the calculation of the received power per resource block from the average of the reference signals. Three secondary nodes with similar channel conditions make use of the individual reference signals for received power calculation per resource block. The final secondary node with best channel conditions, employs MIMO with two antenna arrays of eight antennas. The summary of the results is presented in Table V.

TABLE V. FAIRNESS IMPROVEMENT AND TOTAL CELL THROUGHPUT GAIN.

		Round Robin	Best CQI	Proportional Fair[a]
Fairness Improvement [%]	**μ**	28.91	80.19	24.13
	σ	26.22	40.13	47.34
	MAX	81.18	169.89	104.95
	MIN	-8.15	8.83	-61.72
Total Cell Throughput Gain [%]	**μ**	63.96	41.15	128.52
	σ	35.81	22.80	75.00
	MAX	151.64	127.17	281.88
	MIN	12.54	16.65	1.30

a. Window size: 5 LTE slots.

C. *Dense Deployment Scenario*

The location of the dense deployment scenario is presented in Fig. 10 in Hoskin Avenue near Queen's Park, for a static secondary node synchronized to the eNB with the cell-ID 113 coloured in turquoise. One can also see the interfering cells with the cell-IDs 400, 457, 121 and 120.

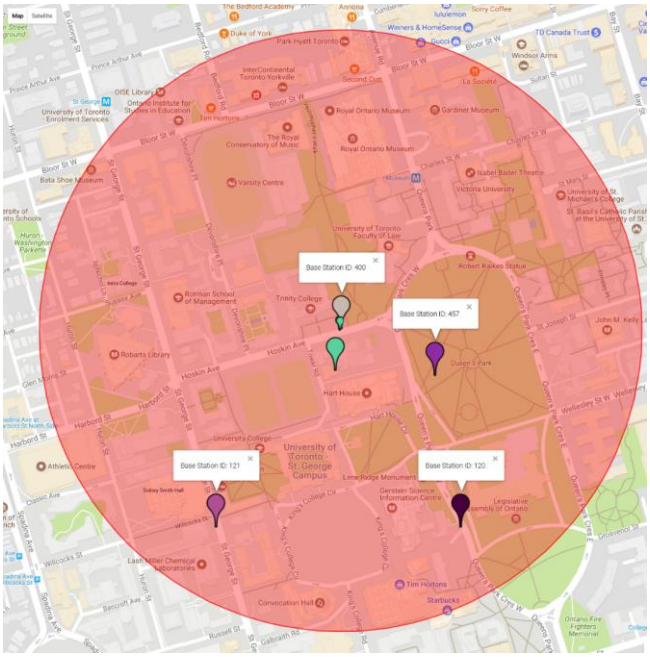

Figure 10 – Dense Deployment Scenario.

From the 21 capture files, no captures followed the three defined categories due to the increased fluctuations in this scenario. For individual reference signals, only four (19 %) captures followed the three categories. The performance of the capture with the most demodulated LTE slots is presented in Fig. 11 for the 7th Reference Signal.

Although the throughput curves have experienced a general decrease due to the added interference, the throughput gain remain fairly similar to the sparse deployment scenario. This promotes the notion that the throughput gain does not depend on the scenario as long as steady channel conditions are verified. The summary of this parameter is found in Table VI.

TABLE VI. DENSE DEPLOYMENT INDIVIDUAL REFERENCE SIGNAL RS_7 PROPOSED SCHEME PERFORMANCE.

	μ	**σ**	**MAX**	**MIN**
$R^{G}_{b,s[\%]}$	64.98	16.91	127.23	36.80

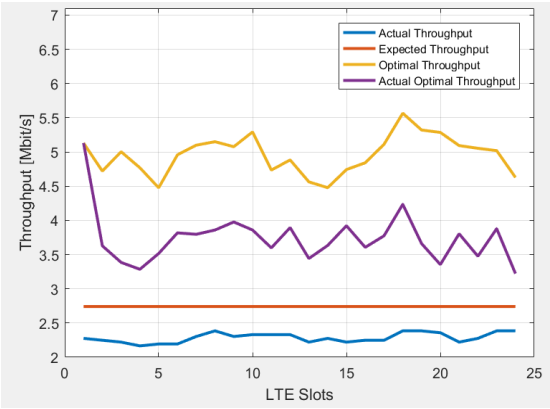

Figure 11 – Dense Deployment Scenario Throughput Curves for Individual Reference Signal RS_7.

VI. CONCLUSIONS

The objective of this thesis was to develop a model to optimize the link between the primary and secondary nodes of a Two-Tier Cellular Network. The optimization is in terms of throughput/capacity by performing Link Adaptation considering multiple MCS for individual resource blocks within a slot. The model is implemented in hardware for data acquisition and software for channel characterization in the secondary node, and, link adaptation and scheduler in the primary node.

Two analyses aim to prove the validity of the proposed scheme over the expected scheme. The first analysis relates to the throughput gain of the proposed scheme, and the second analysis is in terms of the improvements evaluation when one applies three different scheduling algorithms.

The reference scenario pertained to a static secondary node in a sparse deployment, being that a second scenario was built based on this one but considering a dense deployment.

For the files that followed the three defined categories to filter the capture files, the main results on the reference scenario of a sparse deployment revealed a significant improvement of the proposed scheme compared to the expected scheme.

The file with the most demodulated slots, had and average and maximum throughput gain over the expected scheme of 10.23 % and 48.61% for the received power per resource block being based on the individual reference signal RS_7.

Two arrays of eight equally spaced antennas were used to evaluate the improvement when using combining diversity and MIMO. For the reference signal with the best performance, RS_3, as the two arrays had two different performance gains, the obtained results were an average throughput gain of 49.35 % and a maximum value of 105.85 %, although when using MIMO the throughput increased to approximately twice of the value obtained for the two individual arrays.

A fairness improvement of 28.91 %, 80.19 % and 24.13 % and overall cell throughput gain of 63.96 %, 41.15 % and 128.52 % were obtained for the Round Robin, Best CQI and Proportional Fair algorithms for five scheduled secondary nodes with different channel conditions. For the dense deployment scenario, one achieved an average of 64.98 % throughput gain, although most of the capture files did not fit the requirements for the correct performance of the proposed scheme, contrary to the sparse deployment scenario.

Improvements can be integrated to the model in order to enhance its reliability and results. The first improvement refers to the synchronization of the multiple antenna elements. As the equipment possessed imperfections in terms of latency, it led to synchronization issues. One way to improve this problem is to make use of the sub-nanosecond synchronization protocol White Rabbit in BPS. One can also generate the reference clocks and local oscillator frequency externally by using a more accurate clock source, for example a rubidium clock being constantly calibrated over GPS.

In terms of the data acquisition procedure, the next step would be to fix the XGE data acquisition method packet loss rate. One could reduce this loss by reducing the number of XGE connections to the host computer thus reducing its load and improving the rate of received packets. Given that cell location API possesses location inaccuracies, it can lead to possible misinterpretations of what is a sparse or dense deployment influencing the SINR calculation thus creating the need of a more accurate eNB location system.

REFERENCES

[1] 3GPP, LTE-Advanced, http://www.3gpp.org/technologies/keywords-acronyms/97-lte-advanced, November 2016.

[2] N. Rajatheva, and E.S. Sousa, “Hybrid Beamforming for Massive MIMO Backhaul (Working Title)”, University of Toronto, Toronto, Ontario, Canada, Feb. 2016.

[3] BEEcube – A National Instruments Company, *MegaBEE User Manual Revision F02, Firmware v1.1.2*, Santa Clara, CA, USA, 2017.

[4] C. Cox, *An Introduction to LTE: LTE, LTE-Advanced, SAE and 4G Mobile Communications*, Wiley, Chichester, UK, 2012.

[5] S. Saleem, and M. Haneef, “A review of techniques to avoid cross-tier and co-tier interference in femtocell networks”, Journal of Engineering Research, Vol. 4, No. 3, Oct. 2016, pp. 57-84.

[6] M. Simsek, M. Bennis, and I. Guvenc, “Mobility management in HetNets: a learning-based perspective”, EURASIP Journal on Wireless Communications and Networking, Vol. 2015, No.1, Feb. 2015, pp. 1-26.

[7] A. H. Jafari, D. López-Pérez, H. Song, H. Claussen, L. Ho, and J. Zhang, “Small cell backhaul: challenges and prospective solutions”, EURASIP Journal on Wireless Communications and Networking, Vol. 2015, No. 1, Aug. 2015, pp. 1-18.

[8] K. Hosseini, J. Hoydis, S. ten Brink, and M. Debbah, “Massive MIMO and Small Cells: How to Densify Heterogeneous Networks”, in *2013 IEEE International Conference on Communications (ICC)*, Budapest, Hungary, June 2013.

[9] H. Yasuda, A. Kishida, J. Shen, Y. Morihiro, Y. Morioka, S. Suyama, A. Yamada, Y. Okumura, and T. Asai, “A Study on Moving Cell in 5G Cellular System”, in *2015 IEEE 82nd Vehicular Technology Conference (VTC2015-Fall)*, Boston, USA, Sep. 2015.

[10] BEEcube – A National Instruments Company, *Getting started with the MegaBEE Revision F02, Firmware v1.1.2*, Santa Clara, CA, USA, 2017.

[11] BEEcube – A National Instruments Company, *BEEcube Platform Studio Version 5.5 User Manual*, Santa Clara, CA, USA, 2017.

[12] ARM, "AMBA 4 AXI4-Stream Protocol," AXI4-Stream datasheet 2010.

[13] National Instruments, *BPS xGE IP Updates – Prepared for Nokia-US*, Internal Report, Austin, TX, USA, April 2017.

[14] 3GPP, *Technical Specification Group Radio Access Network; Evolved Universal Terrestrial Radio Access (E-UTRA); Physical layer procedures (Release 14)*, TS 36.213, V14.3.0, www.3gpp.org/dynareport/36942.htm, June 2017.

[15] 3GPP, *Technical Specification Group Radio Access Network; Evolved Universal Terrestrial Radio Access (E-UTRA); Radio Frequency (RF) system scenarios (Release 14)*, TR 36.942, V14.0.0, www.3gpp.org/dynareport/36942.htm, March 2017.

[16] 3GPP, *Technical Specification Group Radio Access Network; Evolved Universal Terrestrial Radio Access (E-UTRA); Physical channels and modulation (Release 14)*, TS 36.211, V14.2.0, www.3gpp.org/dynareport/36211.htm, March 2017.

[17] MathWorks, *LTE System Toolbox™ User's Guide*, Natick, MA, USA, 2017.

[18] M. Barberis, and G. Freeland, *Understanding and Demodulating LTE Signals*, Technical Article, MathWorks, Natick, MA, USA, 2015 (https://www.mathworks.com/company/newsletters/articles/understanding-and-demodulating-lte-signals.html).

[19] Mobile Network Guide, *Iphone Field Test Mode*, Powertec Telecommunications Pty Ltd, Australia, 2014 (http://www.mobilenetworkguide.com.au/pdf/Apple-iPhone-Field-Test-Mode.pdf).

[20] LocationAPI, http://locationapi.org/, July 2017.